Journal of Nuclear Materials 389 (2009) 427–431

Contents lists available at ScienceDirect

Journal of Nuclear Materials

journal homepage: www.elsevier.com/locate/jnucmat

Hydrolysis kinetics of lead silicate glass in acid solution

Rafi Ali Rahimi [a,b,*], Sayed Khatibuleslam Sadrnezhaad [a,c], Gholamreza Raisali [d], Amir Hamidi [b]

[a] Materials and Energy Research Center, P.O. Box 14155-4777, Tehran, Iran
[b] Material Research School, Nuclear Science & Technology Research Institute (NSTIR), Atomic Energy Organization of Iran, Moazen Street, Rajaei Shahr, Karaj 31485-498, Iran
[c] Center of Excellence for Production of Advanced Materials, Department of Materials Science and Engineering, Sharif University of Technology, P.O. Box 11365-9466, Tehran, Iran
[d] Radiation Applications Research School, Nuclear Science & Technology Research Institute, Atomic Energy Organization of Iran, End of Karegare Shomali Street, Tehran 11365-3486, Iran

ARTICLE INFO

Article history:
Received 21 November 2008
Accepted 16 February 2009

ABSTRACT

Hydrolysis kinetics of the lead silicate glass (LSG) with 40 mol% PbO in 0.5 N HNO_3 aqueous acid solution was investigated. The surface morphology and the gel layer thickness were studied by scanning electron microscopy (SEM) micrographs. Energy dispersive X-ray spectroscopy (EDS) and inductively coupled plasma spectroscopy (ICP) were used to determine the composition of the gel layer and the aqueous solution, respectively. The silicon content of the dissolution products was determined by using weight-loss data and compositions of the gel layer and the solution. The kinetic parameters were determined using the shrinking-core-model (SCM) for rate controlling step. The activation energy obtained for hydrolysis reaction was $Q_{che} = 56.07$ kJ/mole. The diffusion coefficient of the Pb ions from the gel layer was determined by using its concentration in solution and in LSG. The shrinkage of the sample and the gel layer thickness during dissolution process were determined.

1. Introduction

There have been many investigations about the dissolution of lead and boro-silicate glasses in water and aqueous acid solutions [1–10]. It has become clear that the dissolution of all silicate glasses starts by the ion-exchange reaction and goes on simultaneously by the accomplishment of the ion-exchange reaction in the glass/modifier-depleted film interface and the hydrolysis reaction of the silica in the modifier-depleted/gel layer interface. In LSG glasses, the ion-exchange reaction occurs between H^+ and Pb^{2+} ions [3,4,6,8–10]. Depending on the lead content of the LSG and the concentration of the aqueous acid solution, the ion-exchange reaction results in porous hydrated silica network with one, two, or three siloxane bonds (Si–O–Si bonds between silica tetrahedrons). This dramatically multiplies the active surface area with respect to the initial external surface of the sample [5,11,12]. The hydrolysis reaction is initiated at the weak silica network (silica tetrahedrons with lower siloxane bond) [2,7,13,14] and then goes on to the end.

The modifier elements are dissolved in vast range, but the silica components have limited solubility in solution. By increasing the silicon concentration in solution, re-precipitation of this compound is started [1,5,12–15]. This produces the gel layer on the surface of the LSG glass. The liquid film, gel layer and the modifier depleted layers are the rate limiting steps during dissolution process. They inhibit transfer of components incorporating in ion-exchange (proton and modifier cations) and hydrolysis reactions (water and the hydrated silica molecules) [1,3].

In present study, by using un-reacted core model and the double-stage kinetic modeling procedure in 0.5 N HNO_3 acid solution (pH 0.3), the prevailing step during hydrolysis of the LSG was disclosed [16]. The analytical techniques (SEM–EDS and ICP) were used to determine the morphology of the sample surfaces and the composition of the gel layer and solution. The fractional weight loss of silicon in dissolution products is applied to the software previously developed for simulation of the kinetic processes [17–20]. The thickness of the gel layer was measured by SEM equipment and the sample shrinkage due to the dissolution process was calculated by the silicon amount extracted from the LSG sample and entered into the dissolution products, i.e. the gel layer and the aqueous acid solution.

2. Experimental procedure

Dissolution experiments were carried out on LSG samples with the composition given in Table 1. Rectangular shape samples with $0.015 \times 0.015 \times 0.003$ m^3 dimensions were polished in one side from rough to 3000 mesh, with SiC paper. Their other surfaces covered with anti-acid paste (Sikagard 63N, Sika, and Sweis). The samples were rinsed in 2-propanol for three minutes. They were washed, with deionized water, then dried at 60 °C for 4 h and

---

* Corresponding author. Address: Material Research School, Nuclear Science & Technology Research Institute (NSTIR), Atomic Energy Organization of Iran, Moazen Street, Rajaei Shahr, Karaj 31485-498, Iran.
E-mail addresses: rrahimi@nrcam.org (R.A. Rahimi), sadrnezh@sharif.edu (S.K. Sadrnezhaad), graisali@aeoi.org.ir (G. Raisali), ahamidi@nrcam.org (A. Hamidi).

0022-3115/$ - see front matter © 2009 Elsevier B.V. All rights reserved.
doi:10.1016/j.jnucmat.2009.02.028

Table 1
Compound analyses of the LSG and the gel layer produced on the LSG sample.

Compound substance		As_2O_3	Na_2O	Al_2O_3	SiO_2	ZrO_2	TiO_2	PbO
LSG	(wt%)	0.30	1.60	2.20	24.00	2.40	1.00	68.50
	(mol%)	0.13	2.47	1.60	51.90	2.50	1.60	39.60
Compound substance		As_2O_3	Na_2O	Al_2O_3	SiO_2	ZrO_2	TiO_2	$PbNO_3$
Gel layer	(wt%)	Nil	Nil	1.86	70.19	6.05	0.63	21.26
	(mol%)	Nil	Nil	1.46	93.68	3.94	0.62	0.30

weighed by using (Mettler Toledo AG204) balance with the accuracy of ±0.0001 g. The surface area per volume ratio of 13.3 m^{-1} was exposed to 0.5 N HNO_3 (Ruth, Germany) aqueous acid solution at 0–50 °C for different periods of time.

Sample surfaces were characterized by Philips, XL30 scanning electron microscope equipped with elemental analysis system. The composition of the gel layer was detected by EDS. The solution contents of silicon and lead were determined by inductively coupled plasma analysis (ICP – Perkins Elmer Model Optima 2100 DV) and atomic emission spectrometry.

3. Results and discussion

Table 1 shows the composition of the LSG glass and the gel layer formed on the LSG surface. Table 2 shows silicon and lead contents of the solution after different dissolution periods. It can be seen that the silicon content approaches an almost constant value while that of lead increases with the dissolution time. The near-constant final value of Si indicates establishment of a local equilibrium between the aqueous solution and the gel layer.

The acid solution lead species come from: (a) the selective extraction of lead from the LSG sample according to ion-exchange reaction and (b) the total glass network dissolution process. The diffusion coefficient of Pb through the gel layer is determined by the application of the relation (1) [4]:

$$C^{Pb} = 2\frac{S}{V}C_o^{Pb}\left(\frac{Dt}{\pi}\right)^{1/2}, \tag{1}$$

where C^{Pb} is the concentration of Pb in solution, S/V is the initial surface area of the sample being exposed to the solution per unit volume of the solution, C_o^{Pb} is the concentration of the lead in the LSG sample, D is the diffusion coefficient of the Pb species within the gel layer and t is the dissolution time. With application of the experimental data into the diffusion correlation (1), the diffusion coefficient of Pb in the gel layer is obtained to be 14.2×10^{-16} m^2/s.

After pulling the samples out of the solution and their drying by an oven dryer, the gel layer produced on their surfaces during the dissolution was fractured. The sample with the gel layer on its surface was tilted up to 30° inside the SEM chamber. The micrographs from the thickness and the surface of the gel layer were taken. Fig. 1 shows the micrograph of a typical piece of the gel layer. The angle of the surface of the layer cross section and the upper surface of the gel layer (surface parallel to the interface of the gel layer and the sample) with the micrograph frontier are 60° ($\pi/3$) and 30° ($\pi/6$), respectively, as indicated in the figure. The thickness measured by the SEM picture is, thus, the value of the projection of the gel thickness on the surface of the SEM micrograph. The gel layer thickness can, then, be calculated by using the correlation (2):

$$X = Y\cos(\pi/3), \tag{2}$$

where X is the projection of the gel layer thickness on the surface of the micrograph, and Y is the gel layer thickness.

Fig. 1 compares the morphology of the surface of the LSG sample after dissolution for 6 and 36 h in presence of the gel layer with that after removing of the gel layer. Enhancement of the dissolution time increases the thickness of the gel layer. In sample with no gel layer, a large number of fine cavities distributed on the surface of the sample held for 6 h in the solution are observed. In samples held for 36 h, the cavities are further grown and the surface becomes flattened. Formation of the cavities and grooves is due to extraction of the dissolving elements from the surface of the sample. The modifier content of the LSG components are dissolved into the solution; but the silicon base parts precipitate on the surface of the sample as the gel layer. The compositions of both the solution and the gel layer confirm that the amount of Pb in the solution is high; but its amount in gel layer is low. The zone of the reaction moves into the sample and leaves behind the gel substance. The schematic plot depicted in Fig. 2 indicates the formation of different sub-surface layers during dissolution of the LSG into the acid solution (i.e. liquid film and the gel layer).

Silicon atoms construct the network of the glass but the Pb and other modifying cations are placed in the interstitial positions in the LSG glass. Because of the presence of the large amount of the modifying cations, the intermediate elements such as Zr, Ti and Al incorporate in construction of the glass as network former. Although they incorporate in construction of the glass network, but their amounts in relation to silicon are very low, as it is shown in Table 1. The network of the LSG does not break down by the extraction of the modifiers due to ion-exchange reaction and some intermediates such as Al and Ti by the hydrolysis reaction before silicon. During the hydrolysis of the silica bonds, the glass network breaks down and causes its shrinkage. Using this assumption, the shrinkage of the LSG glass during dissolution process depends on the silicon content of the glass.

The thickness shrinkage of the LSG sample (T_{sh}) and the fractional weight loss of the silicon (X_{Si}) are defined by the following correlation:

$$T_{sh} = \frac{C_{Si} \times V + f'_{Si} \times m'}{d \times f_{Si} \times S}, \tag{3}$$

$$X_{Si} = \frac{C_{Si} \times V + f'_{Si} \times m'}{f_{Si} \times m}, \tag{4}$$

where C_{Si} is the measured mass concentration of the Si in the solution, V is the volume of the solution, (f'_{Si} is the weight fraction of the Si in the gel layer, m' is the mass of the gel layer, d is the density of the LSG sample, f_{Si} is the weight fraction of the Si in the LSG sample, S is the surface area of the sample exposed to the solution and m is the initial mass of the LSG sample.

Table 2
Concentrations of the LSG components dissolved into 0.5 N HNO_3 acid solution at 30 °C. The numbers indicate the mean values for three independent measurements.

Time (s)	Si (kg/m^3)	Pb (kg/m^3)
2.16×10^4	$(5.0 \pm 0.5) \times 10^{-3}$	0.52 ± 0.06
4.32×10^4	$(7.0 \pm 0.5) \times 10^{-3}$	0.72 ± 0.09
6.48×10^4	$(9.0 \pm 0.5) \times 10^{-3}$	0.9 ± 0.1
8.64×10^4	$(9.0 \pm 0.5) \times 10^{-3}$	1.1 ± 0.1
10.80×10^4	$(6.0 \pm 0.5) \times 10^{-3}$	1.2 ± 0.1
12.96×10^4	$(8.0 \pm 0.5) \times 10^{-3}$	1.3 ± 0.1

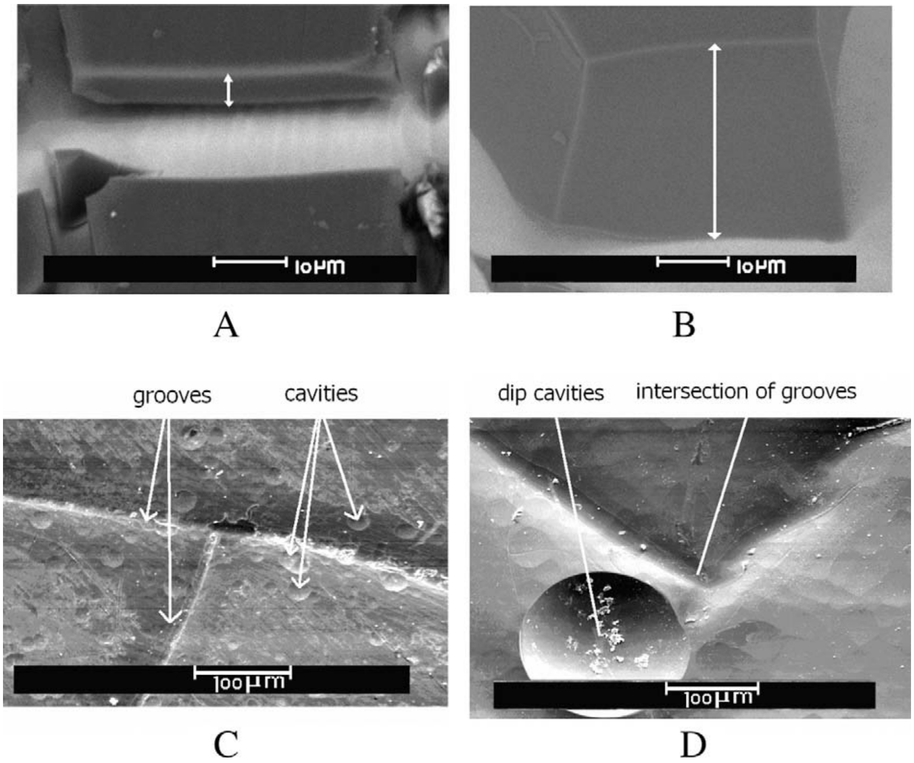

Fig. 1. SEM micrograph of the LSG samples partially dissolved into 0.5 N HNO$_3$ acid solution indicating A: the gel layer thickness after 6 h, B: the gel layer thickness after 36 h, C: the sample surface after 6 h and D: the sample surface after 36 h.

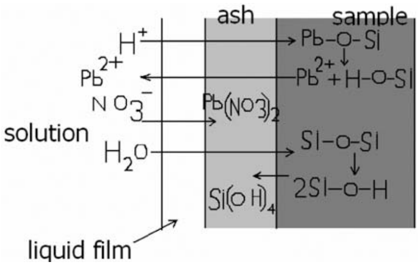

Fig. 2. Schematic representation of the constitution of the liquid film, ash deposit between the interface of the LSG surface and the solution, the mass transfer of the different components between solution and the sample and the accomplishment of the ion-exchange and hydrolysis reactions.

The weight of the silicon in the solution ($C_{si} \times V$) is determined by multiplying the ICP analysis data by the volume of the solution. The weight of the silicon in the gel layer was determined from the gel layer EDS analysis. The weight fraction of the silicon in the gel layer is multiplied by the total weight of the gel layer ($f'_{Si} \times m'$) to determine the amount of Si that goes to the gel layer. The term $C_{Si} \times V + f'_{Si} \times m'$ gives the weight of the silicon being extracted from the glass network during each dissolution test. The relation $d \times f_{Si} \times S$ gives the weight of the silicon extracting the LSG glass per unit length of the thickness. The term $f_{Si} \times m$ gives the total weight of the silicon in the LSG sample which if the LSG totally dissolves, may leave the sample. The correlation (3) gives, therefore, the thickness shrinkage of the sample and the correlation (4) gives the fractional weight of the silicon being extracted from the sample during a test period *t*.

Fig. 3 shows both the variation of the thickness shrinkage of the LSG sample and the thickness of the gel layer produced on the surface of the sample during a dissolution process. The thickness of the gel layer is obtained by measuring of the projection of the gel layer thickness on the surface of the micrographs by the SEM and doing calculation by using the correlation (2). Their values increase linearly with the dissolution time. There is some difference between the amount of the gel thickness and the LSG shrinkage. The gel is constructed by precipitation of the hydrated silicon compounds (silicic acid) when the solution is saturated. The density of the gel layer is 3.00 ± 0.5 g/cm^3 and of the LSG sample is 4.94 ± 0.025 g/cm^3. It seems that the distance between the silicon species in the LSG sample is closer than in the gel layer. The difference between the thickness of the gel layer and shrinkage of the LSG sample at nearly the same amount of silicon depends, therefore, on the packing density of the silicon atoms in the two lattices. It seems that during precipitation, the silicic acid absorbs an excess amount of water molecules from the solution resulting in an increase in the volume of the gel layer.

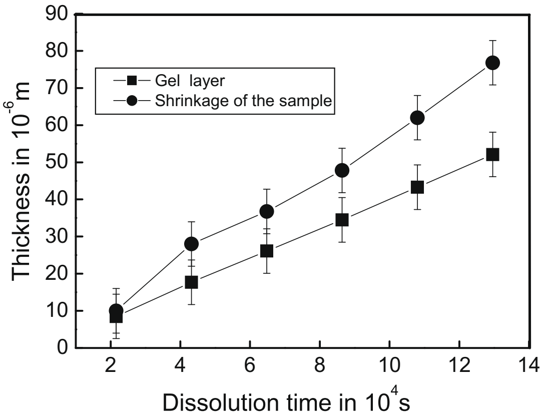

Fig. 3. The thickness shrinkage of the samples and the thickness of the gel layer as a function of time. The thickness shrinkage is obtained from correlation (3) and the thickness of the gel layer is determined from SEM micrographs.

The fractional weight loss of the Si obtained from dissolution experiments is incorporated into the software previously developed for kinetic modeling of the two phase process [18]. The software can evaluate the best-fit total conversion times of all kinetic steps; namely here the chemical reaction (che) and the inter-diffusion (id) of the Si compounds and the water molecules within the gel layer. The time of the reaction is, therefore, determined by the correlation (5):

$$t = \tau_{che} \times X_{Si} + \tau_{id} \times X_{Si}^2, \qquad (5)$$

where τ_{che} and τ_{id} are the total conversion times of the chemical dissolution (hydrolysis reaction) and the internal diffusion through the gel layer, respectively, and X_{Si} is the fractional weight loss of Si during the dissolution. The best-fit curves are determined by minimization of the standard deviation defined by the correlation (6):

$$\sigma^2 = \sum_{i=1}^{n} [t_i - \tau_{\text{che}} \times X_{\text{Si}} - \tau_{\text{id}} \times X_{\text{Si}}^2]^2, \qquad (6)$$

In order to minimize the standard deviation, the derivative of the σ^2 with respect to τ_{che} and τ_{id} must become zero. The weight losses of the Si obtained for different periods of time and temperatures are incorporated into the computer software [18–20] and the results obtained are recorded. The results indicate a chemical reaction step controlling the rate of the process. The fractional weight losses are plotted against time in Fig. 4.

Each silica tetrahedron forms four connections with its neighbors. The molar content of the compounds given in Table 1 indicates that about 50 mol% silica is present in the LSG sample. It shows that two connections of the silica tetrahedrons are from modifiers or intermediates ‘Si–O–C–O–Si’ (C is the modifier or intermediate cation). Two other connections of the silica tetrahedron are direct via siloxane bonds, ‘Si–O–Si’. Before start of the hydrolysis reaction, almost all of the indirect connections during ion-exchange or hydrolysis reactions of intermediates are removed. During the hydrolysis reaction, the water molecules diffuse from solution to the gel layer/glass interface and react with siloxane bond, ‘Si–O–Si’. The hydrolysis reaction of silica is carried out by the reaction (7):

$$\equiv\text{Si}{-}\text{O}{-}\text{Si}\equiv + \text{H}_2\text{O} \leftrightarrow 2\equiv\text{Si}{-}\text{O}{-}\text{H}. \qquad (7)$$

Assuming a pair of the silica tetrahedrons with two direct connections with oxygen atoms and each silica tetrahedron with two hydrated oxygen atoms, the following reaction is then carried out by the water molecules:

$$\text{H}_4\text{Si}_2\text{O}_6 + 2\text{H}_2\text{O} \leftrightarrow 2\text{H}_4\text{SiO}_4. \qquad (8)$$

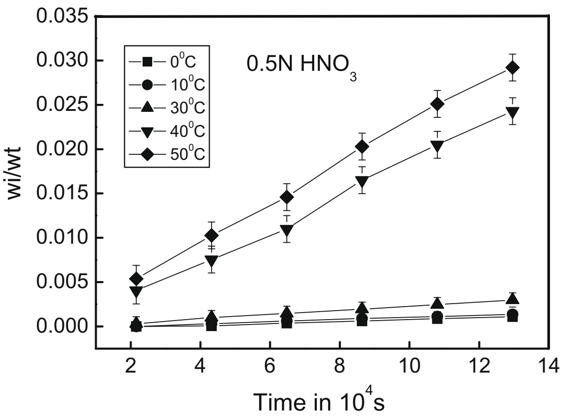

Fig. 4. The leaching fraction of the Si cation from sample surface which maintained inside solution for different times and temperatures, the un-certainty is 10%.

Table 3
Kinetic parameters determined from the experimental data of Si release from lead silicate glass when dissolved in 0.5 N HNO_3.

Temperature (°C)	τ_{che}(s)	k_{che} (m/s)
0	1.33×10^{9}	2.80×10^{-11}
10	9.92×10^{7}	3.76×10^{-11}
30	4.39×10^{7}	8.49×10^{-11}
40	4.66×10^{6}	8.00×10^{-10}
50	3.62×10^{6}	1.03×10^{-9}

Each water molecule breaks one direct silica-tetrahedron connection via hydrolysis reaction. Two water molecules extract, thus, two silicon elements in the form of silicic acid (H_4SiO_4) from the glass network [17]. The silicic acid (H_4SiO_4) molecules transfer back through the gel layer to the gel layer/solution interface. The chemical rate constant of the hydrolysis reaction can be determined by applying the correlation (9) [16]:

$$k_s = \frac{\rho L}{b \tau_{\text{che}} C_A}, \qquad (9)$$

where ρ is the number of the silicon atoms per volume of the LSG sample; L is the thickness of the sample (cm); τ_{che} is the conversion time for chemical reaction; C_A is the concentration of the water molecules in the solution and b is the stoichiometric coefficient of the hydrolysis reaction. It is assumed that each water molecule entering into the glass network achieves equilibrium with the LSG glass to extract one Si atom ($b = 1$). Based on the software calculations and the data plotted in Fig. 4, a chemical mechanism controls the rate of the hydrolysis reaction. The total conversion time and the chemical rate constant of the reaction are determined against temperature for the rate controlling step as given in Table 3. By applying the Arrhenius law, the hydrolysis activation energy is determined from the respective slop of the ln k_{che} versus $1/T$. Its value is $Q_{\text{che}} = 56.07$ kJ/mol.

4. Conclusion

SEM–EDS and ICP analyses are used to characterize the dissolution of LSG samples into 0.5 N HNO_3 acid solution. Analyses of both the gel layer and the acid solution combined with the data obtained from the weight-loss measurements give the silicon content leaving the LSG sample when contacting the aqueous acid solution. SEM micrographs of the surface of the samples show that by increasing the dissolution time, many small cavities in the surface of the sample are produced and grow as further time elapses. Calculations done by computer software illustrate that a chemical reaction is the rate controlling step for hydrolysis of the LSG network into the 0.5 N HNO_3 solution. The thickness shrinkage of the LSG glass and the thickness of the gel layer on the surface of the sample are determined against time. The rate constant and the conversion times of the single controlling step at different temperatures are utilized to determine the activation energy of the controlling step being equal to $Q_{\text{che}} = 56.07$ kJ/mol. The diffusion coefficient of Pb through the gel layer is evaluated to be equal to 14.2×10^{-16} m^2/s.

References

[1] F. Devreux, A. Ledieu, P. Barboux, Y. Minet, J. Non-Cryst. Solids 343 (2004) 13.
[2] M. Melcher, M. Schreiner, J. Non-Cryst. Solids 351 (2005) 1210.
[3] R. Bertoncello, L. Milanes, A. Bouquillon, J.C. Dran, B. Mille, J. Salomon, Appl. Phys. A 79 (2004) 193.
[4] M. Mizuno, M. Takahashi, T. Takaishi, T. Yoko, J. Am. Ceram. Soc. 88 (10) (2005) 2908.
[5] A. Ledieu, F. Devreux, P. Barboux, L. Sicard, O. Spalla, J. Non-Cryst. Solids 343 (2004) 3.
[6] C. Cailleteau, C. weigel, A. Ledieu, P. Barboux, F. Devreux, J. Non-Cryst. Solids 354 (2008) 117.

[7] J. Sheng, S. Luo, B. Tang, Waste Manage. 19 (1999) 401.
[8] C. Bonnet, A. Bouquillon, S. Turrell, V. Deram, B. Mille, J. Salomon, J.H. Thomassin, C. Fiaud, J. Non-Cryst. Solids 323 (2003) 214.
[9] C. Schultz-Münzenberg, W. Meisel, P. Gütlich, J. Non-Cryst. Solids 238 (1998) 83.
[10] A.A. Ahmed, I.M. Youssof, Glass Technol. 38 (1) (1997) 30.
[11] A. Ledieu, F. Devreux, P. Barboux, J. Non-Cryst. Solids 345&346 (2004) 715.
[12] F. Devreux, P. Barboux, J. Nucl. Mater. 298 (2001) 145.
[13] R. Sato, M. Tomozawa, J. Non-Cryst. Solids 343 (2004) 26.
[14] M.I. Ojovan, A. Pankov, W.E. Lee, J. Nucl. Mater. 358 (2006) 57.
[15] F. Devreux, P. Barboux, M. Filoche, B. Sapoval, J. Mater. Sci. 26 (2001) 1331.
[16] O. Levenspiel, Chemical Reactions Engineering, John Wiley, New York, USA, 1972 (Chapter 12).
[17] R. Conradt, J. Am. Ceram. Soc. 91 (3) (2008) 728.
[18] S.K. Sadrnezhaad, A. Gharavi, A. Namazi, IJE Trans. A: Basics 16 (1) (2003) 61.
[19] B. Hashemi, Z. Moghimi, Z.A. Nemati, S.K. Sadrnezhaad, in: Fourth International Symposium: Advances in Refractories for the Metallurgical Industries IV, pp. 581–591.
[20] S.K. Sadrnezhaad, S. Mahshid, B. Hashemi, Z.A. Nemati, J. Am. Ceram. Soc. 89 (4) (2006) 1308.